Tuning *p*-Wave Interactions in an Ultracold Fermi Gas of Atoms

C. A. Regal, C. Ticknor, J. L. Bohn, and D. S. Jin*

*JILA, National Institute of Standards and Technology, and Department of Physics, University of Colorado,
Boulder, Colorado 80309-0440*

We have measured a *p*-wave Feshbach resonance in a single-component, ultracold Fermi gas of ^{40}K atoms. We have used this resonance to enhance the normally suppressed *p*-wave collision cross section to values larger than the background *s*-wave cross section between ^{40}K atoms in different spin states. In addition to the modification of two-body elastic processes, the resonance dramatically enhances three-body inelastic collisional loss.

The ultralow temperature regime accessible in atomic physics is characterized by collision energies so low that centrifugal forces can prevent scattering of atoms with nonzero relative angular momentum. In this case, the atoms collide predominantly via *s*-partial waves ($l = 0$). Even this restricted regime has demonstrated remarkably rich physics in atomic Bose-Einstein condensates [1]. However, the situation is dramatically different for ultracold fermionic atoms. For identical fermions the Pauli exclusion principle forbids *s*-wave collisions. This means the dominant interaction is via *p*-wave collisions ($l = 1$). These collisions are suppressed by centrifugal effects as described by the Wigner threshold law [2,3], which demands that the elastic scattering cross section diminishes with temperature as $\sigma \propto T^2$. For this reason, evaporative cooling of fermions to ultralow temperatures can be achieved only in a mixture of different spin states of the same atom [4,5] or by sympathetic cooling with a different atom [6–9].

However, *p*-wave collisions can become prominent in the presence of a scattering resonance, such as a Feshbach resonance, which occurs when the relative energy of an incident atom pair is nearly degenerate with a quasibound molecular state. In ultracold collisions, Feshbach resonances are useful because the energy at which they occur can be tuned by applying an external magnetic field. For this reason, they have been exploited to measure atomic interactions with great precision [10,11] and to influence the effective interaction between atoms [12]. In all previous cases, Feshbach resonances have been observed only in bosonic species [13–16] or else between two distinct spin states of fermions [17–20].

In this Letter, we report the first measurement of a magnetic-field dependent Feshbach resonance in *p*-wave collisions between ultracold fermionic atoms. This resonance occurs between ^{40}K atoms in the $|F, m_F\rangle = |9/2, -7/2\rangle$ state as predicted in Ref. [21] and results in *p*-wave interactions that are nearly as strong as those from a nearby *s*-wave resonance between the two distinct spin states $|9/2, -7/2\rangle$ and $|9/2, -9/2\rangle$ [17]. We have measured and characterized inelastic collisional losses near this *p*-wave resonance, including loss at the nearby *s*-wave resonance.

The experiments reported here employ previously developed techniques for cooling and spin state manipulation of ^{40}K. Atoms in the $|9/2, 9/2\rangle$ and $|9/2, 7/2\rangle$ states are first held in a magnetic trap and cooled by forced evaporation [4]. The gas is then polarized in the $|9/2, 9/2\rangle$ state and loaded into a far-off resonance optical dipole trap. Adiabatic rapid passage is then used to obtain the desired spin composition [17]. First, the $|9/2, 9/2\rangle$ gas is completely transferred to the $|9/2, -9/2\rangle$ state with a 10 ms rf frequency sweep across all ten spin states at a field of $\sim$30 G. To create a pure $|9/2, -7/2\rangle$ gas, we then move to a higher field, $\sim$80 G, and sweep the magnetic field while applying rf at a fixed frequency to drive the $|9/2, -9/2\rangle$ to $|9/2, -7/2\rangle$ transition.
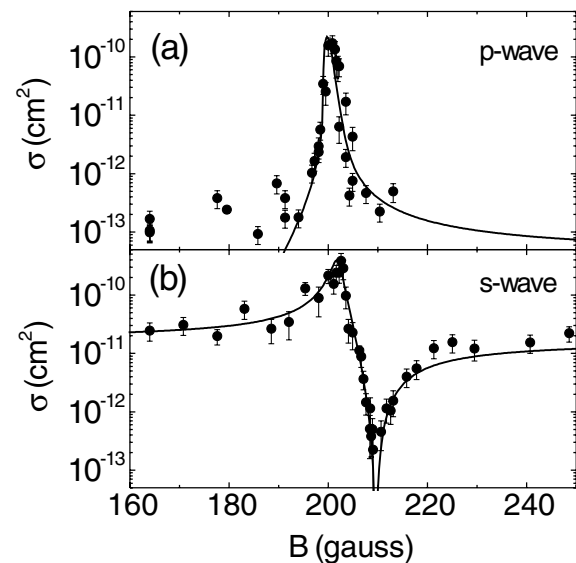

FIG. 1. Magnetic-field Feshbach resonances between ^{40}K atoms in the $|9/2, -7/2\rangle$ state (a) and between atoms in the $|9/2, -9/2\rangle$ and $|9/2, -7/2\rangle$ states (b). The *p*-wave and *s*-wave data were taken at temperatures of 3.2 ± 0.7 μK and 4.4 ± 0.9 μK, respectively (both $T \sim 2T_F$). The lines are based upon our best-fit potassium potentials.

A collision measurement is performed in the optical trap using cross-dimensional rethermalization as described in Ref. [17]. Our optical trap is characterized by transverse frequencies of $\nu_y \approx 1$ kHz and $\nu_x = 1.7\nu_y$ and an axial frequency of $\nu_z = \nu_y/80$. For high collision rates, we use rethermalization between the two transverse directions to ensure that the collision time, not the trap period, defines the rethermalization time τ. We extract the elastic scattering cross section σ via the relation $\frac{1}{\tau} = \frac{2}{\alpha}\langle n \rangle \sigma v$, where the mean relative speed is given by $v = 4\sqrt{k_B T / \pi m}$ and the number density is given by $\langle n \rangle = \frac{1}{N}\int n(\vec{r})^2 d^3\vec{r}$, where N is the total number of atoms. The constant $\alpha = 4.1$ is the calculated average number of binary p-wave collisions per atom required for thermalization [2].

Cross sections for p-wave collisions measured in this way are shown in Fig. 1(a) as a function of the magnetic field. The dominant feature of this resonance is a peak in σ that rises over 3 orders of magnitude above the small background cross section. To the low field side of this peak the effective p-wave interactions are expected to be repulsive, while to the high field side they should be attractive. The zero crossing of the resonance, which is predicted to be ~20 G below the peak, is not observed experimentally. Instead, away from the resonance peak we measure a background value of $\sim 10^{-13}$ cm^2, consistent with a spin state impurity of <0.2%.

For comparison, we also show in Fig. 1(b) the s-wave resonance observed between $|9/2, -7/2\rangle$ and $|9/2, -9/2\rangle$ atoms. This plot includes data from Ref. [17] as well as additional measurements near the peak of the resonance. The presence of non-negligible off-resonant scattering in the s-wave case makes the characteristic asymmetry of the Fano line shape more apparent for this resonance than for the p-wave resonance [22]. Note that, despite the difference in the background p-wave and s-wave cross sections, the strengths of these partial waves become comparable on resonance.

For these data, the magnetic-field values B were calibrated using rf-driven Zeeman transitions and have a systematic uncertainty of $\pm 0.1\%$. The error bars in σ are dominated by measurement uncertainties in τ. In addition, σ has an overall systematic uncertainty of $\pm 50\%$ that comes from measurements of N. The curves in Fig. 1 are best-fit theory calculations using the standard close-coupling theory of ultracold collisions and are appropriately thermally averaged [23,24]. The relative position of the s-wave and p-wave resonances depends sensitively on the C_6 van der Waals coefficient. This arises from the role that the van der Waals potential plays in setting the centrifugal barrier height for p-wave collisions. Measuring the separation in magnetic field of the two resonances therefore enables us to determine a value of $C_6 = 3927 \pm 50$ atomic units, in good agreement with the predicted value of $C_6 = 3897 \pm 15$ [25]. The values

for a_t and a_s obtained from the simultaneous fit are consistent with the values quoted in Ref. [17].

One striking feature of Fig. 1 is the close proximity of the p-wave resonance to the previously reported s-wave resonance in ^{40}K. At zero temperature, the two resonances are separated in field by only 2.8 ± 0.8 G. This result is apparently purely coincidental. By artificially varying either C_6, a_s, or a_t for potassium, we have calculated that the resonances both shift to different values of the field. For example, if the singlet scattering length had been $165a_0$ instead of $104a_0$, the resonances would have been separated by ~70 G.

To view the temperature dependence of the p-wave resonance, we plot in Fig. 2 the elastic scattering cross section for $|9/2, -7/2\rangle$ collisions at two temperatures. For this plot the data from Fig. 1 are divided into two temperature sets and compared to thermally averaged theoretical results based on our best-fit potassium potentials. We observe that the resonance line shape in Fig. 2 displays an asymmetry characteristic of near-threshold resonances, as is seen in photoassociation spectroscopy [26]. The onset of the resonance at 198.8 ± 0.5 G is sharp and relatively insensitive to temperature; this is the field value at which a high-lying molecular bound state appears as a low-energy resonance and can be accessed at any temperature. In contrast, the high field tail of the asymmetric peak is a strong function of temperature.

In addition to elastic scattering, inelastic collision rates can be altered at Feshbach resonances. For the combinations of spin states we are studying, spin-exchange collisions are energetically forbidden at these temperatures and magnetic-field strengths. Thus, for the p-wave resonance the dominant two-body inelastic collision process is the reaction $|9/2, -7/2\rangle + |9/2, -7/2\rangle \rightarrow |9/2, -7/2\rangle + |9/2, -9/2\rangle$, driven by a comparatively weak magnetic dipole interaction. On the other hand, for the s-wave resonance, the $|9/2, -7/2\rangle$ and $|9/2, -9/2\rangle$ states are distinguished by being the two lowest-energy states of the ^{40}K atom at the magnetic fields in this experiment; they are therefore immune to any
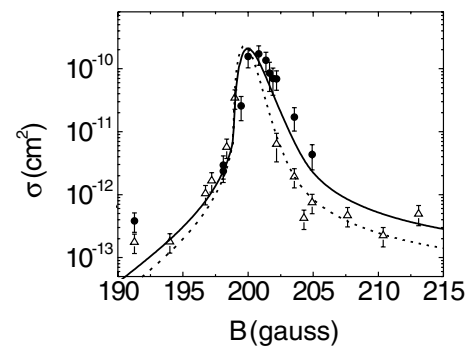
FIG. 2. Temperature dependence of the p-wave elastic collision cross section. The two temperatures sets are 3.7 ± 0.5 μK ($\bullet$) and 2.7 ± 0.3 μK ($\triangle$).

two-body losses associated with the s-wave resonance. Further, by symmetry there can be no p-wave Feshbach resonance between atoms in these two spin states of ^{40}K.

Significant trap loss can also arise from three-body collisions, in which two atoms recombine into a bound molecular state, while the third atom carries away the binding energy. For bosons these collisions can cause a significant limitation to trap lifetimes near a Feshbach resonance [10,13]. For ultracold fermions three-body interactions can be suppressed by Fermi statistics [27]. However, this statistical suppression does not exist at a scattering resonance, and thus three-body loss is expected near the peaks of our Feshbach resonances.

We have probed inelastic collisions near the p-wave resonance by tracking depletion of trapped atoms. Figure 3(a) presents the inelastic collisional loss near the p-wave resonance for a gas of $|9/2, -7/2\rangle$ atoms. Here we assume the loss is dominated by three-body processes and characterize the loss in terms of a three-body atom loss rate L_3. Because of our uncertainty in measured N ($\pm 50\%$), all quoted values for L_3 have a systematic uncertainty of a factor of 3. Near the resonance the loss rate varies by orders of magnitude, just as the elastic rate does, with rate constants comparable to those seen for bosons [28,29]. The loss rate also shows the characteristic asymmetry arising from threshold effects, as seen in the elastic two-body cross section.

Because this p-wave resonance is likely to affect inelastic collision processes at the nearby s-wave resonance, we have also measured atom loss rates for a gas containing an equal mixture of $|9/2, -9/2\rangle$

and $|9/2, -7/2\rangle$ atoms. Here we examined the atom loss across the peaks of both the p-wave and s-wave resonances, whose zero temperature resonance positions are located at 198.8 ± 0.5 G and 201.6 ± 0.6 G, respectively. As shown in Fig. 3(b), the loss at a temperature of 2.8 ± 0.4 μK is a broad peak that encompasses both resonances. At a lower temperature of 1.25 ± 0.10 μK, the loss appears as two distinct peaks, one at the same magnetic field as the p-wave loss peak and the other near the peak of the s-wave resonance.

In general, three-body loss processes in a Fermi gas are influenced by Fermi exchange symmetry. With two distinct spin states present, a three-body collision may involve either a pair of atoms in one spin state and the third atom in the other, or else all three atoms in the same spin state. Away from resonance, this difference combined with Fermi exchange symmetry alters the threshold behavior of three-body collisions [27]. On resonance, the influence of this dynamics remains to be explored [30].

We have also performed a study of the density dependence of the observed loss at the p-wave resonance through measurements of loss of atoms in time as the density of the gas changed by an order of magnitude. The loss trends were analyzed with the following rate equation [28]:

$$\frac{dN}{dt} = -L_2\langle n\rangle N - L_3\langle n^2\rangle N - \frac{N}{\tau_0}. \tag{1}$$

Here $\langle n^2\rangle = \frac{1}{N}\int n(\vec{r})^3 d^3\vec{r}$, and $\tau_0 = 32$ s describes the exponential lifetime of atoms in our optical trap. The time evolution of the size of the gas is included in the density terms. For a field of 198.8 G, we plot in Fig. 4 the number loss dN/dt as a function of the atomic density $\langle n\rangle$. The solid and dashed lines in Fig. 4 are best fits assuming exclusively three-body loss ($L_2 = 0$) or two-body loss ($L_3 = 0$), respectively. The data at this field are clearly consistent with three-body, but not two-body, losses. Figure 5 presents the results of this procedure at various field values across the p-wave resonance. Here we compare the two-body and three-body loss at a density typical
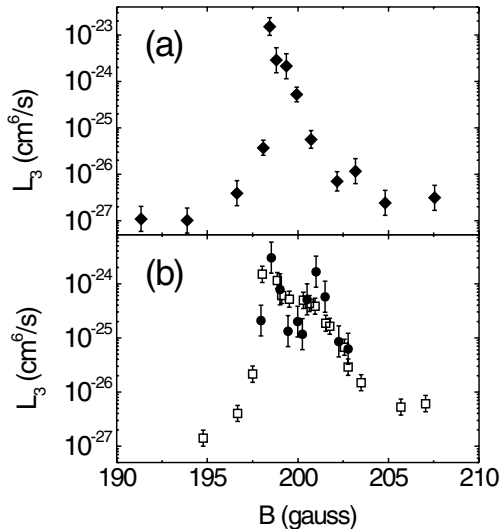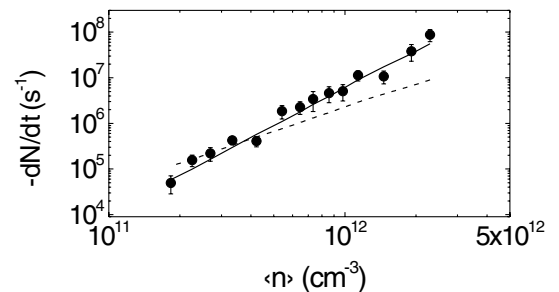
FIG. 3. Resonant three-body loss for a gas of atoms in the (a) $|9/2, -7/2\rangle$ state and (b) $|9/2, -7/2\rangle$ and $|9/2, -9/2\rangle$ states. The data in (a) were taken at a temperature of 2.4 ± 0.8 μK, while the data in (b) were taken at 1.25 ± 0.10 μK ($\bullet$) and 2.8 ± 0.4 μK ($\square$). The error bars are determined from scatter among repeated loss measurements.

FIG. 4. Density dependence of $|9/2, -7/2\rangle$ atom loss at $B = 198.8$ G. The lines are results of best-fit curves that assume either exclusively two-body loss (dashed line) or exclusively three-body loss (solid line).
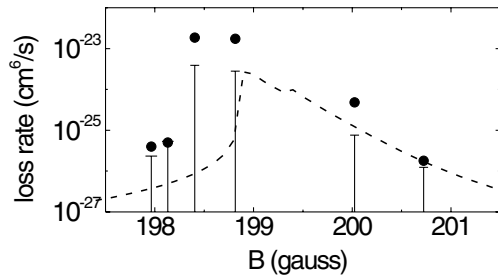

FIG. 5. Comparison of three-body and two-body loss of $|9/2, -7/2\rangle$ atoms across the p-wave resonance at a temperature of 2.7 ± 0.7 μK. Data shown are L_3 (●) and an experimental upper limit on the value of L_2 (solid lines). For comparison to L_3, L_2 is divided by a typical density of $\langle n \rangle = 3 \times 10^{12}$ cm^{-3}. The dashed line is the result of a close-coupling calculation of the two-body inelastic atom loss rate.

of the initial density of our cloud, $\langle n \rangle = 3 \times 10^{12}$ cm^{-3}. At the peak of the Feshbach resonance, the three-body loss clearly dominates over the limiting value of L_2. For comparison, we also plot the theoretically expected two-body loss rate, which lies within the measured upper limit for this rate. A similar analysis of the loss of $|9/2, -7/2\rangle$ and $|9/2, -9/2\rangle$ atoms near the s-wave peak shows that this loss process is also predominantly three-body at our typical densities.

In conclusion, we have observed a p-wave Feshbach resonance for ultracold fermions and characterized both the elastic and inelastic processes near this resonance in ^{40}K. The observed elastic cross sections for the combination of the p-wave and nearby s-wave resonances constrain C_6 for potassium. Further, the modification of the elastic cross sections provided by these resonances yields ultracold fermions with tunable interactions. In particular, the availability of both p-wave and s-wave resonance offers the opportunity to study strong interactions between both identical and nonidentical fermions. Among the most interesting prospects for such strong interactions is driving Cooper pairing of fermionic atoms [31–33]. However, three-body interactions result in dramatic losses at these ^{40}K resonances. Thus, understanding on-resonance threshold behavior of the three-body collisions involved will be critical to utilizing these resonances to achieve a strongly interacting Fermi gas of atoms.

———————————

*Quantum Physics Division, National Institute of Standards and Technology.

[1] F. Dalfovo, S. Giorgini, L. P. Pitaevskii, and S. Stringari, Rev. Mod. Phys. **71**, 463 (1999).

[2] B. DeMarco, J. L. Bohn, J. P. Burke, Jr., M. Holland, and D. S. Jin, Phys. Rev. Lett. **82**, 4208 (1999).

[3] H. R. Sadeghpour *et al.*, J. Phys. B **33**, R93 (2000).

[4] B. DeMarco and D. S. Jin, Science **285**, 1703 (1999).

[5] S. R. Granade, M. E. Gehm, K. M. O'Hara, and J. E. Thomas, Phys. Rev. Lett. **88**, 120405 (2002).

[6] A. G. Truscott, K. E. Strecker, W. I. McAlexander, G. B. Partridge, and R. G. Hulet, Science **291**, 2570 (2001).

[7] F. Schreck *et al.*, Phys. Rev. A **64**, 011402 (2001).

[8] Z. Hadzibabic *et al.*, Phys. Rev. Lett. **88**, 160401 (2002).

[9] G. Roati, F. Riboli, G. Modugno, and M. Inguscio, Phys. Rev. Lett. **89**, 150403 (2002).

[10] J. L. Roberts, J. P. Burke, Jr., N. R. Claussen, S. L. Cornish, E. A. Donley, and C. E. Wieman, Phys. Rev. A **64**, 024702 (2001).

[11] C. Chin, V. Vuletic, A. J. Kerman, and S. Chu, Phys. Rev. Lett. **85**, 2717 (2000).

[12] J. L. Roberts, N. R. Claussen, S. L. Cornish, E. A. Donley, E. A. Cornell, and C. E. Wieman, Phys. Rev. Lett. **86**, 4211 (2001).

[13] S. Inouye, M. R. Anders, J. Stenger, H.-J. Miesner, D. M. Stamper-Kurn, and W. Ketterle, Nature (London) **392**, 151 (1998).

[14] Ph. Courteille, R. S. Freeland, D. J. Heinzen, F. A. van Abeelen, and B. J. Verhaar, Phys. Rev. Lett. **81**, 69 (1998).

[15] J. L. Roberts, N. R. Claussen, J. P. Burke, Jr., C. H. Greene, E. A. Cornell, and C. E. Wieman, Phys. Rev. Lett. **81**, 5109 (1998).

[16] V. Vuletic, A. J. Kerman, C. Chin, and S. Chu, Phys. Rev. Lett. **82**, 1406 (1999).

[17] T. Loftus, C. A. Regal, C. Ticknor, J. L. Bohn, and D. S. Jin, Phys. Rev. Lett. **88**, 173201 (2002).

[18] S. Jochim *et al.*, Phys. Rev. Lett. **89**, 273202 (2002).

[19] K. M. O'Hara *et al.*, Phys. Rev. A **66**, 041401 (2002).

[20] K. Dieckmann, C. A. Stan, S. Gupta, Z. Hadzibabic, C. H. Schunck, and W. Ketterle, Phys. Rev. Lett. **89**, 203201 (2002).

[21] J. L. Bohn, Phys. Rev. A **61**, 053409 (2000).

[22] U. Fano, Phys. Rev. **124**, 1866 (1961).

[23] For the p wave we fit only points with $\sigma > 10^{-12}$ cm^2.

[24] J. P. Burke, Jr. *et al.*, Phys. Rev. A **60**, 4417 (1999).

[25] A. Dereviako, W. R. Johnson, M. S. Safronova, and J. F. Babb, Phys. Rev. Lett. **82**, 3589 (1999).

[26] R. Napolitano, J. Weiner, C. J. Williams, and P. S. Julienne, Phys. Rev. Lett. **73**, 1352 (1994).

[27] B. D. Esry, C. H. Greene, and H. Suno, Phys. Rev. A **65**, 010705 (2001).

[28] J. L. Roberts, N. R. Claussen, S. L. Cornish, and C. E. Wieman, Phys. Rev. Lett. **85**, 728 (2000).

[29] J. Stenger, S. Inouye, M. R. Andrews, H.-J. Miesner, D. M. Stamper-Kurn, and W. Ketterle, Phys. Rev. Lett. **82**, 2422 (1999).

[30] H. Suno, B. D. Esry, and Chris H. Greene, Phys. Rev. Lett. **90**, 053202 (2003).

[31] H. T. C. Stoof, M. Houbiers, C. A. Sackett, and R. G. Hulet, Phys. Rev. Lett. **76**, 10 (1996).

[32] M. Holland, S. J. J. M. F. Kokkelmans, M. L. Chiofalo, and R. Walser, Phys. Rev. Lett. **87**, 120406 (2001).

[33] E. Timmermans, K. Furuya, P. W. Milloni, and A. K. Kerman, Phys. Lett. A **285**, 228 (2001).